



HAL
open science

Piezoelectric and Ferroelectric Properties of Lead-free 0.9(Na_{0.97}K_{0.03}NbO₃)- 0.1BaTiO₃ Solid Solution

S Sasikumar, R Saravanan, S Saravanakumar

► **To cite this version:**

S Sasikumar, R Saravanan, S Saravanakumar. Piezoelectric and Ferroelectric Properties of Lead-free 0.9(Na_{0.97}K_{0.03}NbO₃)- 0.1BaTiO₃ Solid Solution . Mechanics, Materials Science & Engineering MMSE Journal. Open Access, 2017, 9, 10.2412/mmse.47.30.332 . hal-01503665

HAL Id: hal-01503665

<https://hal.science/hal-01503665>

Submitted on 7 Apr 2017

HAL is a multi-disciplinary open access archive for the deposit and dissemination of scientific research documents, whether they are published or not. The documents may come from teaching and research institutions in France or abroad, or from public or private research centers.

L'archive ouverte pluridisciplinaire **HAL**, est destinée au dépôt et à la diffusion de documents scientifiques de niveau recherche, publiés ou non, émanant des établissements d'enseignement et de recherche français ou étrangers, des laboratoires publics ou privés.



Distributed under a Creative Commons Attribution 4.0 International License

Piezoelectric and Ferroelectric Properties of Lead-free $0.9(\text{Na}_{0.97}\text{K}_{0.03}\text{NbO}_3)$ - 0.1BaTiO_3 Solid Solution

S. Sasikumar¹, R. Saravanan¹, S. Saravanakumar²

1 – Research Centre and Post Graduate Department of Physics, The Madura College, Madurai - 625 011, Tamil Nadu, India

2 – Department of Physics, Kalasalingam University, Krishnankoil, Viruthunagar - 626 126, Tamil Nadu, India



DOI 10.2412/mmse.47.30.332 provided by Seo4U.link

Keywords: ceramics, piezoelectricity, X-ray diffraction, electronic structure.

ABSTRACT. Lead-free piezoelectric $0.9(\text{Na}_{0.97}\text{K}_{0.03}\text{NbO}_3)$ - 0.1BaTiO_3 ceramic has been synthesized using conventional solid-state reaction method. The results of X-ray diffraction analysis (XRD) show that the prepared sample displays typical perovskite structure with tetragonal space group $P4mm$. The crystal structure of $0.9(\text{Na}_{0.97}\text{K}_{0.03}\text{NbO}_3)$ - 0.1BaTiO_3 powder was determined by Rietveld refinement analysis. The charge density distribution of the prepared sample has been investigated by using maximum entropy method. The optical band gap of the solid solution has been investigated using UV-visible spectroscopy (UV-Vis). Scanning electron microscopic (SEM) measurements were performed to study the surface morphology. The elemental composition of the $0.9(\text{Na}_{0.97}\text{K}_{0.03}\text{NbO}_3)$ - 0.1BaTiO_3 sample was analyzed by energy-dispersive X-ray (EDS) spectrometer. The ferroelectric nature of the sample has been determined through polarization and electric field hysteresis measurements.

Introduction. Lead-based piezoelectric materials like PZT (lead zirconate titanate) are the most widely used piezoelectric materials for its superior piezoelectric properties, but these Pb-based systems are highly toxic and volatile causing serious environmental hazards [1,2]. Recently, considerable research has been intensified on lead-free based piezoelectric materials [3]. In this context, (Na, K) NbO_3 based ceramic systems are emerging as promising candidates for replacement of lead-based ceramics due to their excellent piezoelectric properties, high Curie temperature and environmental friendliness. Pure NKN ceramics are difficult to synthesize using the solid state reaction method due to the evaporation of K_2O and Na_2O at high temperatures and degradation of resistivity and the piezoelectric properties. It is also very difficult to control the evaporation of Na_2O and K_2O by muffling. So, to synthesize the pure NKN samples and optimizations have been adapted by adjusting the Na/K ratio in A site of perovskite structure [4]. Several research works have been carried out by doping the extrinsic materials to increase the piezoelectric properties of NKN-based ceramic materials. Dopants such as LiTaO_3 [5], CuO [6], ZnO , LiSbO_3 [7], LiNbO_3 [8], BaTiO_3 [9], SrTiO_3 [10], CaTiO_3 [11], AgTaO_3 [12], Fe_2O_3 [13], and Sb_2O_5 [14] have been added to NKN-based ceramics to form new NKN-based ceramic systems. In the present work, we report $0.9(\text{Na}_{0.97}\text{K}_{0.03}\text{NbO}_3)$ - 0.1BaTiO_3 ceramic was synthesized by solid-state reaction method. The ferroelectric and piezoelectric properties of $0.9(\text{Na}_{0.97}\text{K}_{0.03}\text{NbO}_3)$ - 0.1BaTiO_3 ceramic were analyzed through charge density studies.

Experimental. Solid solution sample of $0.9(\text{Na}_{0.97}\text{K}_{0.03}\text{NbO}_3)$ - 0.1BaTiO_3 was prepared by conventional solid-state reaction method. Na_2CO_3 (99.99%), K_2CO_3 (99.99%), Nb_2O_5 (99.99%), BaCO_3 (9.99%) and TiO_2 (99.99%) were used as starting materials. The raw powders were weighed in the stoichiometric ratio of $0.9(\text{Na}_{0.97}\text{K}_{0.03}\text{NbO}_3)$ - 0.1BaTiO_3 and mixed through ball milling using agate balls for 2 h. Then, the powder was calcined at 950°C for 4 h. The powder was then pressed

into discs (pellets) using a hydraulic press with 12 mm diameter and 1 mm thickness. These pellets were then finally sintered at 1250 °C for 2 h. The prepared solid solution was characterized using various techniques. The crystal structure and phase formation were confirmed by analyzing X-ray diffraction pattern of the sample obtained by X-ray diffractometer (Bruker AXS D8 Advance) in a wide range of angles (10° to 120°) with a scanning step size 0.02° at room temperature using CuK α radiation ($\lambda = 1.54056 \text{ \AA}$). Surface morphological and the compositional study was carried out using a scanning electron microscope (SEM) (JEOL JSM-6390LV) equipped with energy dispersive X-ray spectrometer (EDS) (JEOL JED-2300). Optical band gap analysis was carried out using Varian, Cary 5000 spectrophotometer in the wavelength range of 200-2000 nm. Piezoelectric constant (d_{33}) of the sample was measured using a Piezo- d_{33} meter (SINOCERA, YE2730A d_{33} meter), after poling the pellet of the prepared ceramic sample in silicone oil at temperature 80 °C under 3-4 kV/mm for 30 min with no leakage current. P-E hysteresis loop was obtained by Radiant Precision Workstation ferroelectric testing system at room temperature.

Results and discussion.

Structural analysis

Fig. 1(a) shows the powder X-ray diffraction pattern of the $0.9(\text{Na}_{0.97}\text{K}_{0.03}\text{NbO}_3)\text{-}0.1\text{BaTiO}_3$ solid solution. No peak corresponding to any secondary phase was observed in the X-ray diffraction pattern. It can be concluded that the $\text{Na}_{0.97}\text{K}_{0.03}\text{NbO}_3$ and BaTiO_3 ceramics form a homogeneous perovskite ABO_3 structure. The crystal structure of $0.9(\text{Na}_{0.97}\text{K}_{0.03}\text{NbO}_3)\text{-}0.1\text{BaTiO}_3$ ceramic possess tetragonal with $P4mm$ symmetry. The inset of fig. 1(a) shows the splitting of the 46° diffraction peak (200) into (200) and (002) indicates tetragonal symmetry. In our work, the Rietveld refinement [15] was performed through the JANA 2006 program [16]. The fitted profile is shown in fig. 1(b). The lattice parameters and unit cell volume were calculated through of Rietveld refinement and are as presented in table 1.

Table 1. Structural parameters.

Parameters	Values
a=b (Å)	3.9471(8)
c (Å)	3.9283(7)
Space group	$P4mm$
Volume (Å ³)	61.30(2)
Density (gm/cc)	4.45(1)
R _P (%)	6.30
R _{obs} (%)	2.13
*F ₍₀₀₀₎	79

*Number of electrons in the unit cell

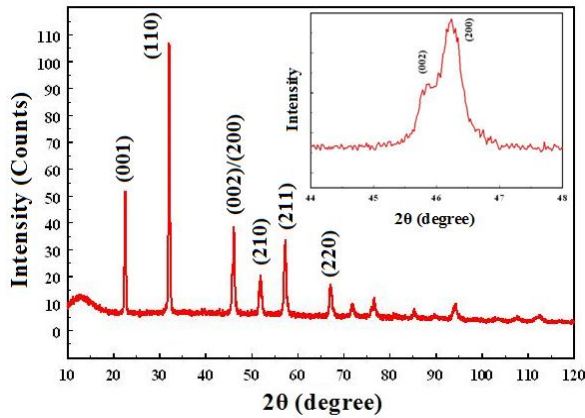


Fig. 1. a) X-ray diffraction pattern of $0.9(\text{Na}_{0.97}\text{K}_{0.03}\text{NbO}_3)-0.1\text{BaTiO}_3$.

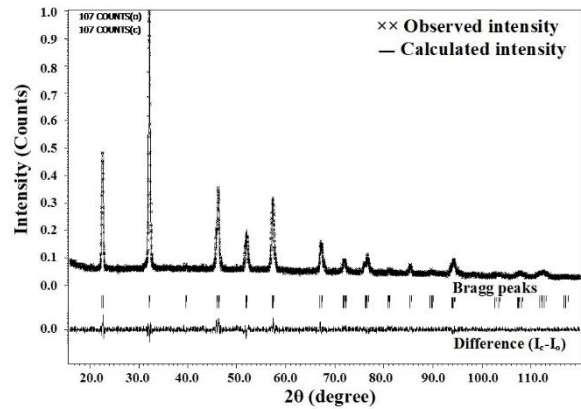


Fig. 1. b) Fitted powder XRD profile.

Microstructural properties. To study the influence of BaTiO_3 content on the microstructure of $\text{Na}_{0.97}\text{K}_{0.03}\text{NbO}_3$ ceramics, their surface morphology was characterized by the scanning electron microscopy. Fig. 2 shows the corresponding SEM pattern of $0.9(\text{Na}_{0.97}\text{K}_{0.03}\text{NbO}_3)-0.1\text{BaTiO}_3$ sample. It can be seen that the SEM particles are finely distributed without much agglomeration. Fig. 3 show the EDS spectra for the prepared samples. The result indicates that the constituent ions are present in the respective samples in expected proportion. No additional impurities are detected in the EDS spectrum. The numerical values of the percentages of atom and weight are given in table 2. It is interesting to note that the preparation condition completely favors the formation of mixed BaTiO_3 and allow us to study the effect of the properties of the $\text{Na}_{0.97}\text{K}_{0.03}\text{NbO}_3$.

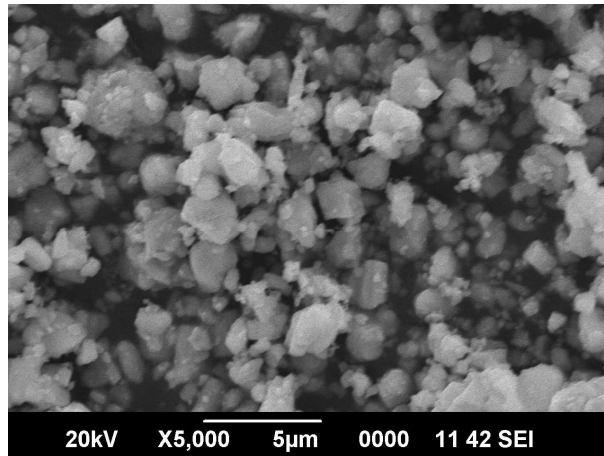


Fig. 2. SEM image.

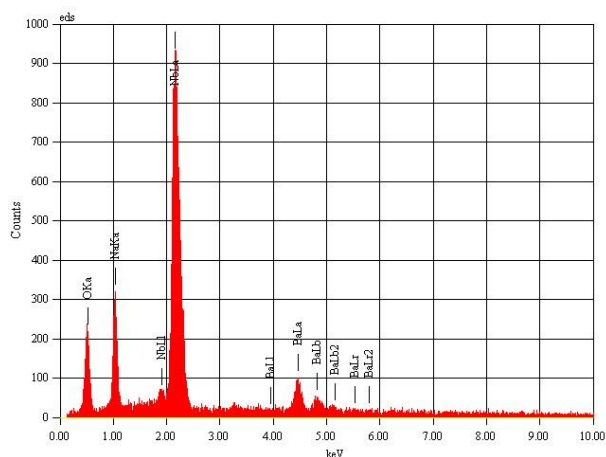


Fig. 3. EDS spectra.

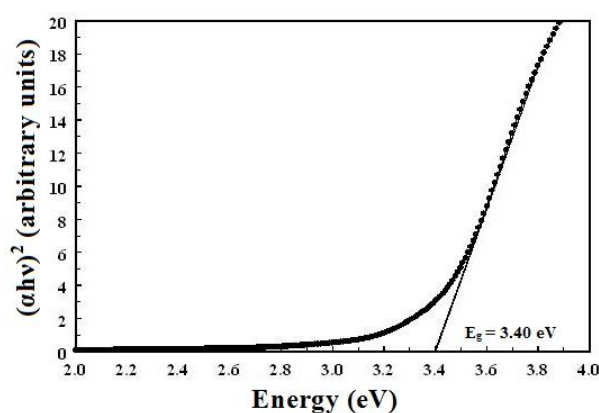


Fig. 4. UV-Visible plot.

Table 2. EDS elemental composition for $0.9(\text{Na}_{0.97}\text{K}_{0.03}\text{NbO}_3)-0.1\text{BaTiO}_3$.

Weight (Wt %)						Atomic (At %)					
Na	K	Nb	Ba	Ti	O	Na	K	Nb	Ba	Ti	O
13.06	0.77	47.79	9.37	1.51	28.51	18.87	1.36	17.41	2.31	1.07	60.33

Optical properties. The band gap energy of the prepared sample $0.9(\text{Na}_{0.97}\text{K}_{0.03}\text{NbO}_3)-0.1\text{BaTiO}_3$, ceramic was evaluated using UV-visible spectra. Optical band gap was determined using the equation proposed by Wood and Tauc [17], $\alpha h\nu = A(h\nu - E_g)^n$ where A is a constant, α is the absorbance, $h\nu$ is photon energy, E_g is energy band gap, $n=1/2$ for direct band gap materials and $n=2$ for indirect band gap materials. Using Tauc's relation, a graph is drawn with the energy value in X-axis and $(\alpha h\nu)^2$ in Y-axis. By extrapolating the linear portion of the curve as shown in fig. 4, the band gap values are estimated to be 3.40 eV.

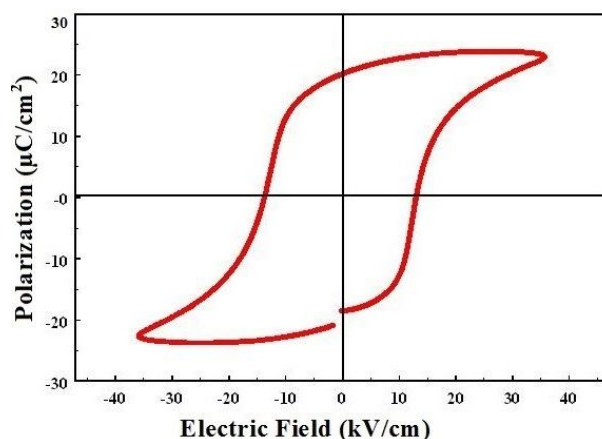


Fig.5. Ferroelectric P-E hysteresis loops of $0.9(\text{Na}_{0.97}\text{K}_{0.03}\text{NbO}_3)\text{-}0.1\text{BaTiO}_3$ ceramics at room temperature

Ferroelectric and piezoelectric properties. The ferroelectric properties of the $0.9(\text{Na}_{0.97}\text{K}_{0.03}\text{NbO}_3)\text{-}0.1\text{BaTiO}_3$ ceramic was investigated in terms of their P-E hysteresis loop at room temperature as shown in fig. 5. The maximum polarization (P_{max}), remnant polarization (P_{r}) and coercive field (E_{c}) values observed for the sample are $23.83 \mu\text{C}/\text{cm}^2$, $20.12 \mu\text{C}/\text{cm}^2$, $1.3 \text{ kV}/\text{mm}$, respectively. The piezoelectric coefficient (d_{33}) of polarized $0.9(\text{Na}_{0.97}\text{K}_{0.03}\text{NbO}_3)\text{-}0.1\text{BaTiO}_3$ ceramic proves strong piezoelectric responses of the prepared ceramics. The polarized ceramic $0.9(\text{Na}_{0.97}\text{K}_{0.03}\text{NbO}_3)\text{-}0.1\text{BaTiO}_3$ have piezoelectric d_{33} value of $110 \text{ pC}/\text{N}$. This implies an essential relation between the piezoelectric property and the ferroelectric nature of the $0.9(\text{Na}_{0.97}\text{K}_{0.03}\text{NbO}_3)\text{-}0.1\text{BaTiO}_3$ ceramic.

Charge density analysis from maximum entropy method. Maximum entropy method (MEM) [18] is an important and accurate technique to deal the electron density distribution in the unit cell because of their probabilistic approach. Also, it only needs a minimum amount of information from the observed XRD spectra and it yields least biased information. This method is packaged by the software PRactice Iterative MEM Analyses (PRIMA) [19]. The structure factors extracted from Rietveld refinement technique [15] were used for this study. The electron density distribution in the unit cell was constructed through the PRIMA [19] software. The MEM calculation for $0.9(\text{Na}_{0.97}\text{K}_{0.03}\text{NbO}_3)\text{-}0.1\text{BaTiO}_3$ ceramic was carried out using $64 \times 64 \times 64$ pixels along a, b and c axes of the tetragonal lattice. The results are visualized using visualization software VESTA (Visualization for Electronic and Structural Analysis) [19]. Three-dimensional charge density distributions in the unit cell of $0.9(\text{Na}_{0.97}\text{K}_{0.03}\text{NbO}_3)\text{-}0.1\text{BaTiO}_3$ is constructed with similar iso-surface levels of $1 \text{ e}/\text{\AA}^3$ and are presented in fig. 6 (a) and (c) with (001) and (002) planes shaded which gives a better view of how the charges are spatially distributed between constituent atoms inside the unit cell. Fig. 6 (b) and (d) shows that the two-dimensional charge density distributions on (001) and (002) planes with the enlarged view of electron density distribution around Na, Nb and O atoms. It is evident that the contour lines are faded away from the boundary of the Na and O atoms (fig. 6(b)) which reveal that there is no charge accumulation at the middle of the bond. This qualitatively confirms that between the Na and O atoms, the bond is ionic in nature. But, as far as the two-dimensional electron density map for the Nb-O bond in the (002) plane is concerned, it is clear from the fig. 6(d) that there is an increase of charges in the bonding region between the two atoms which authenticate that Nb-O bond is covalent in nature. These results are quantitatively analyzed by plotting one-dimensional charge density profile along Na-O and Nb-O, which are shown in fig. 7 (a) and (b). The mid bond electron density values are tabulated in table 3. We have attempted to correlate the piezoelectric response of $0.9(\text{Na}_{0.97}\text{K}_{0.03}\text{NbO}_3)\text{-}0.1\text{BaTiO}_3$ with charge density distributions in the host lattice. Then Nb-O bond is facilitating the vibrations in the NbO_6 octahedrons. The mid bond electron density value between Nb and O atoms is $1.0445 \text{ e}/\text{\AA}^3$ (table 3). The higher value of mid-bond electron density confirms covalent character between Nb and O atoms. The presence of more charges in the mid-bond region

of Nb-O atoms may be attributed to the enhanced ferroelectric and piezoelectric properties. The maximum polarization and d_{33} values for prepared sample are $23.83 \mu\text{C cm}^{-2}$ and 110 pC N^{-1} . XRD results show that the prepared sample possesses tetragonal structure that might be due to the increase of off-centered octahedral Nb ion displacement. This may lead to enhanced ferroelectric and piezoelectric properties of the composition.

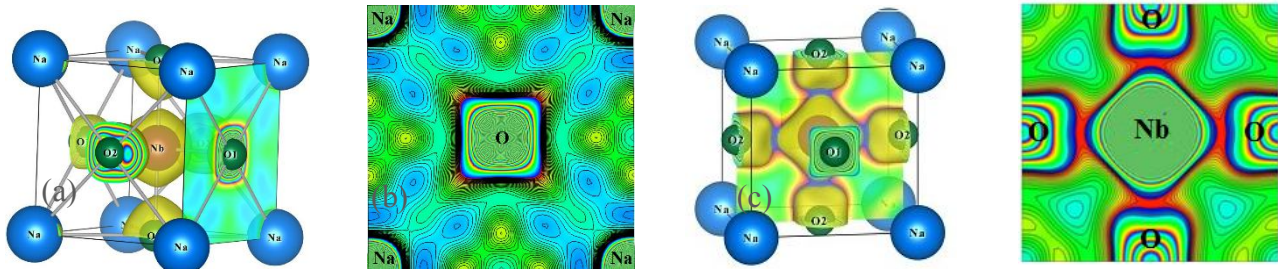


Fig. 6. a) 3D unit cells of $0.9(\text{Na}_{0.97}\text{K}_{0.03}\text{NbO}_3)-0.1\text{BaTiO}_3$ with a) (001) and c) (002) planes shaded. Two dimensional electron density distribution on b) (001) and d) (002) planes for $0.9(\text{Na}_{0.97}\text{K}_{0.03}\text{NbO}_3)-0.1\text{BaTiO}_3$.

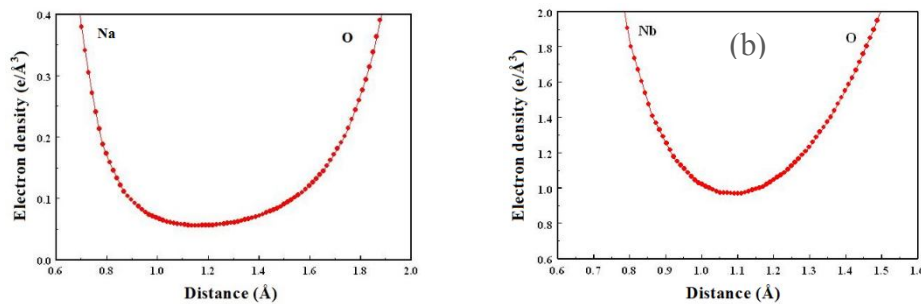


Fig. 7. One dimensional electron density profiles along a) Na and O b) Nb and O atoms.

Table 3. Bond lengths and mid bond electron densities for Na-O, Nb-O bonds.

Bonding			
Na-O		Nb-O	
Bond length (Å)	Mid bond electron density ($\text{e}/\text{Å}^3$)	Bond length (Å)	Mid bond electron density ($\text{e}/\text{Å}^3$)
2.7901	0.0695	1.9741	1.0445

Summary. $0.9(\text{Na}_{0.97}\text{K}_{0.03}\text{NbO}_3)-0.1\text{BaTiO}_3$ ceramic has been prepared by solid state reaction method. The phase and structural properties have been analyzed by X-ray diffraction in the $\text{Na}_{0.97}\text{K}_{0.03}\text{NbO}_3$ ceramic by doping BaTiO_3 . Piezoelectric, ferroelectric and charge derived properties of the grown sample have been correlated. The covalent nature between Nb and O ions was revealed from charge density studies, which are responsible for the piezoelectric properties of $0.9(\text{Na}_{0.97}\text{K}_{0.03}\text{NbO}_3)-0.1\text{BaTiO}_3$. The band gap for the prepared sample was estimated by UV-visible spectra and it found to be 3.40 eV. The morphological study was performed by scanning electron microscopy. The elemental composition of the grown sample was also analyzed by using EDS spectrum.

References

- [1] Y. Saito, H. Takao, T. Tani, T.T. Nonoyama, K. Takatori, T. Homma, T. Nagaya and M. Nakamura, (2004) Lead-free piezoceramics. *Nature* 432, 84. DOI:10.1038/nature03028
- [2] T.R. Shrout and S.J. Zhang, (2007) Lead-free piezoelectric ceramics: Alternatives for PZT? *J Electroceram.* 19, 113. DOI: 10.1007/s10832-007-9047-0
- [3] W. Liu, X. Ren, (2009) Large piezoelectric effect in Pb-free ceramics, *Large Piezoelectric Effect in Pb-Free Ceramics Phys. Rev. Lett.* 103. 257602. DOI:doi.org/10.1103/PhysRevLett.103.257602
- [4] Q. Zhang, B. Zhang, H. Li, P. Shang, (2010) Effects of Na/K ratio on the phase structure and electrical properties of $\text{Na}_x\text{K}_{1-x}\text{NbO}_3$ lead-free piezoelectric ceramics, *Rare Metals.* 29, 220-225. DOI: 10.1007/s12598-010-0038-y
- [5] M.R. Yang, C.-S. Hong, C.C. Tsai, S.Y. Chu, (2009) Effect of sintering temperature on the piezoelectric and ferroelectric characteristics of CuO doped $0.95(\text{Na}_{0.5}\text{K}_{0.5})\text{NbO}_3\text{-}0.05\text{LiTaO}_3$ ceramics, *J. Alloys Compd.* 488, 169-173. DOI:10.1016/j.jallcom.2009.07.174
- [6] H.Y. Park, I.T. Seo, J.H. Choi, S. Nahm, H.G. Lee, (2010) Low-temperature sintering and piezoelectric properties of $(\text{Na}_{0.5}\text{K}_{0.5})\text{NbO}_3$ lead-free piezoelectric ceramics, *J. Am. Ceram. Soc.* 93, 36-39. DOI: 10.1111/j.1551-2916.2009.03359.x
- [7] G.Z. Zang, J.F. Wang, H.C. Chen, W.B. Su, C.M. Wang, P. Qi, B.Q. Ming, J. Du, L.M. Zheng, S. Zhang, T.R. Shrout, (2006) Perovskite $(\text{Na}_{0.5}\text{K}_{0.5})_{1-x}(\text{LiSb})_x\text{Nb}_{1-x}\text{O}_3$ lead-free piezoceramics, *Appl. phys. Lett.* 88, 212908. DOI: 10.1063/1.2206554
- [8] J. Zeng, Y. Zhang, L. Zheng, G. Li, Q. Yin, (2009) Enhanced ferroelectric properties of potassium sodium niobate ceramics modified by small amount of $\text{K}_3\text{Li}_2\text{Nb}_5\text{O}_{15}$, *J. Am. Ceram. Soc.* 92, 752-754. DOI: 10.1111/j.1551-2916.2008.02921.x
- [9] D. Lin, K.W. Kwok, H.L.W. Chan, (2007) Structure, dielectric, and piezoelectric properties of CuO -doped $\text{K}_{0.5}\text{Na}_{0.5}\text{NbO}_3\text{-BaTiO}_3$ lead-free ceramics, *J. Appl. Phys.* 102, 074113. DOI: 10.1063/1.2787164
- [10] R.C. Chang, S.Y. Chu, Y.P. Wong, Y.F. Lin, C.S. Hong, (2007) Properties of $(\text{Na}_{0.5}\text{K}_{0.5})\text{NbO}_3\text{-SrTiO}_3$ based lead-free ceramics and surface acoustic wave devices, *Sens. Actuators A: Phys.* 136, 267–272. DOI:10.1016/j.sna.2006.11.002
- [11] R.C. Chang, S.Y. Chu, Y.F. Lin, C.S. Hong, Y.P. Wong, (2007) An investigation of $(\text{Na}_{0.5}\text{K}_{0.5})\text{NbO}_3\text{-CaTiO}_3$ based lead-free ceramics and surface acoustic wave devices, *J. Eur. Ceram. Soc.* 27, 4453-4460. DOI:10.1016/j.sna.2006.11.002
- [12] Y. Wang, L. Qibin, F. Zhao, (2010) Phase transition behavior and electrical properties of $[(\text{K}_{0.50}\text{Na}_{0.50})_{1-x}\text{Ag}_x](\text{Nb}_{1-x}\text{Ta}_x)\text{O}_3$ lead-free ceramics, *J. Alloys Compd.* 489, 175-178. DOI:10.1016/j.jallcom.2009.09.047
- [13] R. Zuo, Z. Xu, L. Li, (2008) Dielectric and piezoelectric properties of Fe_2O_3 -doped $(\text{Na}_{0.5}\text{K}_{0.5})_{0.96}\text{Li}_{0.04}\text{Nb}_{0.86}\text{Ta}_{0.1}\text{Sb}_{0.04}\text{O}_3$ lead-free ceramics, *J. Phys. Chem. Solids* 69, 1728-1732. DOI:10.1016/j.jpcs.2008.01.003
- [14] Q. Zhang, B.-P. Zhang, H.-T. Li, P.-P. Shang, (2010) Effects of Sb content on electrical properties of lead-free piezoelectric $[(\text{Na}_{0.535}\text{K}_{0.480})_{0.942}\text{-Li}_{0.058}](\text{Nb}_{1-x}\text{Sb}_x)\text{O}_3$ ceramics, *J. Alloys Compd.* 490, 260-263. DOI:10.1016/j.jallcom.2009.09.172
- [15] H.M. Rietveld, (1969) A Profile Refinement Method for Nuclear and Magnetic, *J. Appl. Cryst.* 2, 65-71. doi.org/10.1107/S0021889869006558
- [16] V. Petříček, M. Dušek, L. Palatinus, Jana 2006. *The Crystallographic Computing System*, Institute of Physics, Prague, Czech Republic, 2006.
- [17] D.L. Wood, J. Tauc, (1972) Weak absorption tails in amorphous semiconductors. *Phys. Rev. B* 5, 3144.

- [18] D.M. Collins, (1982) Electron density images from imperfect data by iterative entropy maximization, *Nature* 298, 49-51.
- [19] K. Momma, F. Izumi, *Commission on Crystallogr. Comput., IUCr Newslett.*, No.7, 106 (2006).

Cite the paper

S. Sasikumar, R. Saravanan, S. Saravanakumar, (2017). [Piezoelectric and Ferroelectric Properties of Lead-free 0.9\(Na0.97Ko.03NbO3\)-0.1BaTiO3 Solid Solution](#). *Mechanics, Materials Science & Engineering*, Vol 9. Doi [10.2412/mmse.47.30.332](#)